Ultra-sensitive transition-edge sensors for the Background Limited Infrared/Sub-mm Spectrograph (BLISS)

A.D. Beyer, M.E. Kenyon, P. M. Echternach, T. Chui, B.-H. Eom, P.K. Day, J.J. Bock, W.A. Holmes, C.M. Bradford

Department of physics, California Institute of Technology/Jet Propulsion Laboratory, 1200 E. California Blvd., 91125 Pasadena, CA U.S.A.

We report progress in fabricating ultra-sensitive superconducting transition-edge sensors (TESs) for BLISS. BLISS is a suite of grating spectrometers covering 35-433μm with R~700 cooled to 50mK that is proposed to fly on the Japanese space telescope SPICA. The detector arrays for BLISS are TES bolometers readout with a time domain SQUID multiplexer. The required noise equivalent power (NEP) for BLISS is NEP=10^{-19} W/Hz$^{1/2}$ with an ultimate goal of NEP= 5 × 10^{-20} W/Hz$^{1/2}$ to achieve background limited noise performance. The required and goal response times are τ=150ms and τ=50ms respectively to achieve the NEP at the required and goal optical chop frequency 1-5Hz. We measured prototype BLISS arrays and have achieved NEP=6 × 10^{-18} W/Hz$^{1/2}$ and τ=1.4ms with a Ti TES (T_C=565mK) and NEP~2.5 × 10^{-19} W/Hz$^{1/2}$ and τ~4.5ms with an Ir TES (T_C=130mK). Dark power for these tests is estimated at 1-5fW.

PACS numbers: 85.25.Pb; 95.85.Gn; 95.85.Fm; 63.22.+m

1. INTRODUCTION

The next generation of space-borne infrared (IR)/sub-mm instruments will study the epoch of reionization and the first galaxies with cryogenic telescopes offering greatly improved spectroscopic sensitivity compared to current missions such as Herschel and SOFIA. A possible instrument to fly on the JAXA satellite-mission SPICA is our Background Limited IR/Sub-mm Spectrograph (BLISS). BLISS will provide 1-2×10^{-20} W/m^2 (3σ, 1 hour) line sensitivity for spectroscopy from 35-433μm in 6 bands.

To meet the needed performance specifications, BLISS requires fast, ultra-sensitive bolometers with noise equivalent power NEP=10^{-19}W/Hz$^{1/2}$ and response time τ=150ms. The goal for BLISS is to exceed the required NEP and τ with NEP=5×10^{-20} W/Hz$^{1/2}$ and τ=50ms. To cover the full band with two beams at the target resolving power, 4224 TESs are required in

total. We use membrane-isolated transition-edge sensors (TESs) as the most likely candidate for near-term achievement of these specifications.

The expected NEP for such TESs is given by[1]

$$NEP = \sqrt{\gamma 4 k_B T_C^2 G} \; ; \quad \gamma = \frac{n+1}{2n+3}\left(\frac{1-(1-t)^{2n+3}}{1-(1-t)^{n+1}}\right) \tag{1}$$

where $t=1-T_b/T_C$, T_b is the base temperature of operation, T_C is the transition temperature of the superconducting thermistor, k_B is Boltzmann's constant, G is thermal conductance of the TES support beams and $G \sim T^n$. The thermal time constant $\tau_0 = C/G$, where C is the heat capacity of the TES absorber and thermistor. In voltage-biased electrothermal feedback operation[2], τ is decreased according to

$$\tau = \frac{\tau_0}{1 + P_J \alpha / G T_C} \tag{2}$$

where P_J is the operating point Joule power and $\alpha = d\log R / d\log T$. τ is expected to be about 20 times smaller than τ_0 for real materials used in BLISS[3]. BLISS will use a 50mK space-qualified cryocooler and we are baselining bilayer thermistors with T_C=65mK.

In previous studies[4], we utilized Johnson noise Thermometry Devices (JTDs) to measure G and C as a function of temperature and found that $G \sim T^{1/2}$ near T_C=65mK for the Si_xN_y support beam geometries we use. The base requirements of BLISS dictate we need G= 60fW/K and C=180fJ/K, whereas the goal levels will require G=15fW/K and C=15fJ/K. Our JTD measurements suggest we can meet the requirement levels for BLISS and are approaching the goal NEP from Eq. (1). Our thrust is now to demonstrate such performance with actual electrical measurements.

In this paper, we present electrical performance measurements of arrays of TESs with BLISS straight-beam geometries (1mm × 0.4μm × 0.25μm) and meander-beam geometries (2mm × 0.4μm × 0.25μm) using higher-T_C transitions in the presence of our 0.9 fW (minimum) excess load.

2. ARRAYS AND EXPERIMENTAL SETUP

We fabricated 1×32 arrays of BLISS TESs[5] using Ir (T_C=130mK) and Ti (T_C=565mK) as superconducting thermistors and characterized the arrays using NIST SQUID multiplexing (MUX) chips[6] and multi-channel electronics (MCE) from the University of British Columbia.

Ultra-sensitive transition-edge sensors for the Background Limited Infrared/Sub-mm Spectrograph (BLISS) Instrument

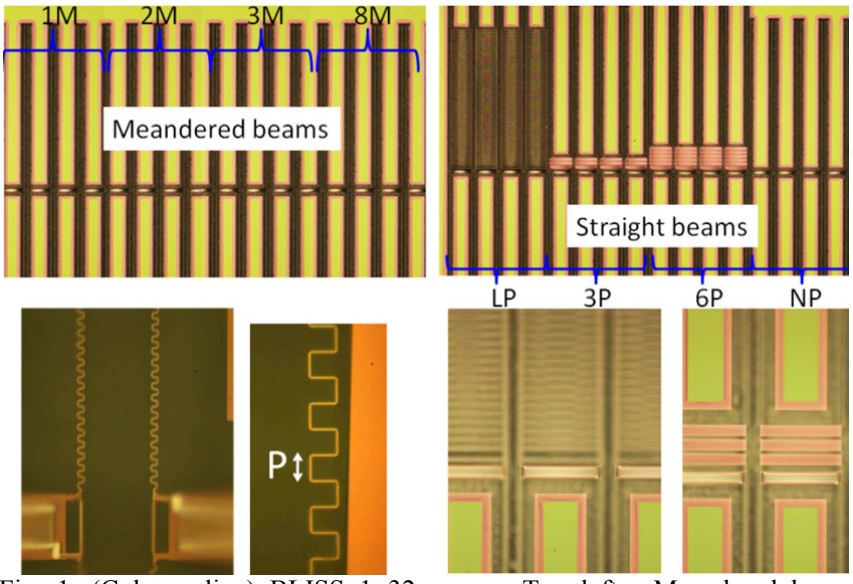

Fig. 1. (Color online) BLISS 1×32 array: Top left: Meandered beam TESs—1M (P=1μm), 2M (P=2μm), 3M (P=3.5μm), 8M (P=8μm). Top right: straight-beam TESs—LP (ladder-plank absorber), 3P (3 plank absorber), 6P (6 plank absorber), NP (no absorber). Bottom left: Zoomed image showing meander beams and meander pitch P. Bottom right: Zoomed image of LP (left) and 3P (right) absorbers.

Our apparatus utilizes a 2-stage adiabatic demagnetization refrigerator (ADR). One stage cools a 1K Al shield surrounding our 2nd, mK-stage which reaches a base temperature of 43mK. Each 1×32 TES array is surrounded by a light-tight Nb box sealed with indium gaskets.

A 1×32 arrays of TESs is shown in Fig. 1. The top row of Fig. 1 shows optical microscope images of the different types of TESs in the array. The left side of the array employs meandered support beams with varying square pitch P of the meander (bottom left of Fig. 1) and without absorbers. The right half of the array has straight beam TESs with varying absorbers (e.g. right bottom of Fig. 1). For simplicity in fabrication, we have not yet employed metalized beams along the absorbers to ensure strong thermal coupling between the absorbers and thermistors. To a first approximation, the straight beams TESs operate without coupling to absorbers. The TESs are released from the silicon underneath them using XeF_2.

Our light-tight Nb boxes for arrays contain two compartments with one for the array and the other for filtering connections to the array. The

compartments are separated by a Nb partition sealed with an indium gasket. Two filters were tested: (1) a π-filter with roll-off at ~40MHz and (2) an L/R filter with roll-off near 150kHz (see Ref. [5]). The filter and the light-tight box reduced the dark electrical and optical power P_{dark} from coupling to our TESs. A challenge for BLISS is to reduce P_{dark} to the order of 10aW.

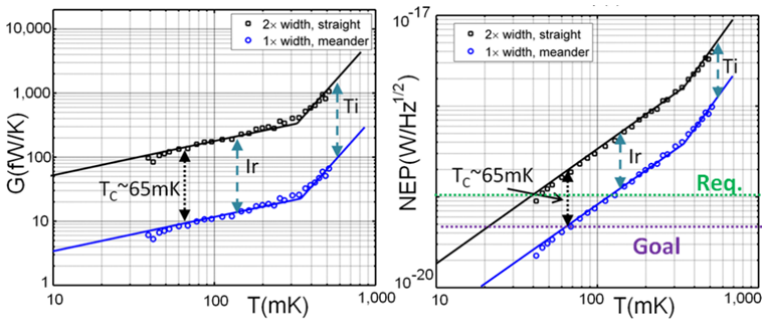

Fig. 2. (Color online) Expected G (left) and NEP (right) values vs. temperature for BLISS TESs based on JTD measurements (More details, see Ref. [3]).

We achieved P_{dark} =0.9-5fW for the ADR testbed used here (see Table 1). Half of the minimum P_{dark}=450aW in our ADR would already suppress the apparent T_C of a G=15fW/K, T_C=65mK TES to ~30mK, which is below our base temperature. (Three unreleased devices were wired up on each 1×32 array to measure T_C without reduction of the apparent T_C due to P_{dark}.) We are developing new filters and will further seal our Nb boxes with indium and Eccosorb in an attempt to further lower P_{dark}. Higher P_{dark} means that we must measure TESs with larger T_C in order to make measurements, which is why we have used Ti and Ir for our thermistors here.

Based on the measured G vs. T for our JTDs with 1mm × 0.4μm×0.25μm beams, we can predict the values of G and NEP that will be observed in the arrays. Assuming that the beam widths can vary up to double the assumed width (up to 0.8μm), we show the upper and lower limit expectations for G and NEP in Fig. 2.

4. RESULTS AND DISCUSSION

We show representative: load curves and power vs. temperature plots for our Ir devices in Fig. 3; and NEP and τ measurements for Ir TESs operated within the transition region in Fig. 4. A strong 1/f signal with knee near 5Hz, which we believe arises from our readout, is apparent in the NEP plots. All TESs exhibit excess noise near ~1/(2πτ), and we conjecture that

the strong 1/f and excess noise occurring at smaller frequencies, due to larger τ values in meander TESs, conspire to produce measured NEPs greater than predicted. Increasing T_b and the voltage bias reduces the excess noise marginally. The γ factor seems to be irrelevant for Ti and Ir meander TESs, disagreeing with the predicted values in Table 1 from Eq. (1).

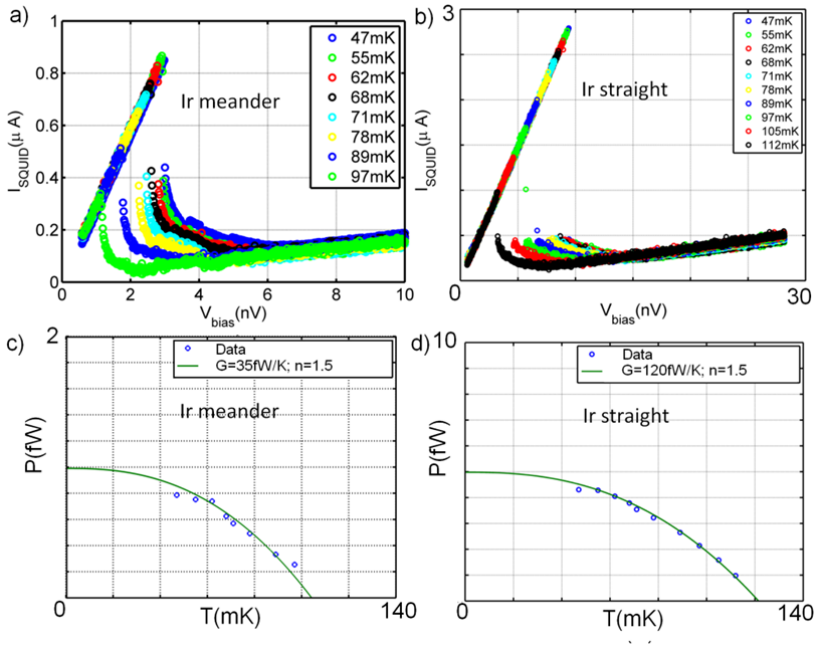

Fig. 3. (Color online) a) Load curves used to generate plot in b). b) Power vs T plots for an Ir meander TES. The data (blue circles) and fit (green line) are shown, with the fit using G=35fW/K, $G\sim T^{1.5}$,and P_{dark}=0.9fW. c) Load curves used to generate plot in d). d) Power vs T plots for an Ir straight beam TES. The data (blue circles) and fit (green line) are shown, with the fit using G=120fW/K, $G\sim T^{1.5}$,and P_{dark}=1.5fW.

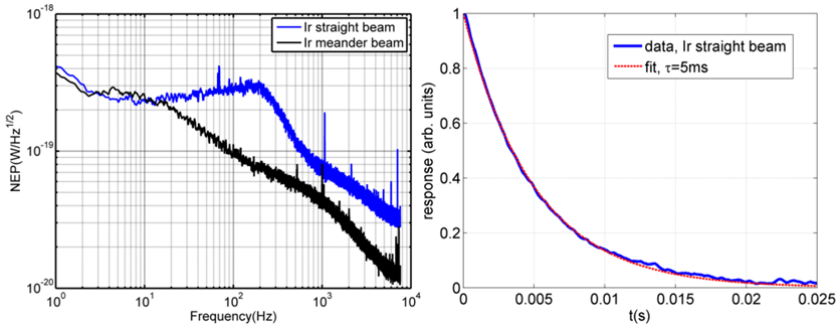

Fig. 4. (Color online) Left: Measured NEPs for the lowest NEP Ir devices. NEP is calculated from the measured noise equivalent current times the voltage bias. The device response is only valid for frequency<1/(2πτ) Right: Representative τ measurement with the TESs biased within the transition.

A summary of our results for various Ti and Ir TESs is shown in Table 1. TESs employing the π-filter (40MHz bandwidth) are shaded grey in Table 1, whereas TESs using the L/R filter (150kHz bandwidth) are not shaded. The L/R filtered TESs exhibit smaller P_{dark}=0.9-2.5fW than the π-filtered TESs (P_{dark}=4-4.8fW) suggesting P_{dark} is more due to electrical stray power than optical stray power. The values of γ increase as n decreases for Ir films.

Material (T_c)	Type	G (fW/K)	n ($G\sim T^n$)	P_{dark} (fW)	γ (50mK)	NEP_{exp} ($10^{-19}W/Hz^{1/2}$)	NEP_{meas} ($10^{-19}W/Hz^{1/2}$)	τ (ms)	τ_{Band5} (ms)
Ir (130mK)	3M	35	0.5	0.9	0.62	1.4	2.5	7.9	131
Ir (130mK)	2M	30	0.5	0.9	0.62	1.3	2.0	16.5	274
Ir (130mK)	2M	30	0.5	0.9	0.62	1.3	2.0	30.2	502
Ir (130mK)	1M	35	1.5	0.9	0.56	1.4	2.0	32.3	537
Ir (130mK)	NP	110	0.5	2.5	0.62	2.5	2.5	4.8	79
Ir (130mK)	3P	115	1.5	2.0	0.56	2.5	2.5	5.2	86
Ir (130mK)	6P	120	1.5	1.5	0.56	2.5	2.5	5.0	83
Ir (130mK)	6P	120	1.5	1.5	0.56	2.5	2.5	4.7	77
Ir (130mK)	6P	110	1.5	1.0	0.56	2.4	2.5	4.5	76
Ir (130mK)	6P	110	1.5	1.0	0.56	2.4	2.5	4.7	78
Ir (130mK)	6P	120	0.5	4.8	0.62	2.6	2.6	1.3	22
Ir (130mK)	6P	110	0.5	4.8	0.62	2.5	2.9	3.7	61
Ir (130mK)	NP	140	0.5	4.0	0.62	2.8	2.9	1.5	24
Ir (130mK)	NP	100	0.5	4.6	0.62	2.4	2.5	3.3	55
Ti(565mK)	NP	11000	3	NA	0.81	125.4	200	*	*
Ti(565mK)	3P	1450	3	NA	0.81	45.5	60	*	*
Ti(565mK)	LP	1450	3	NA	0.81	45.5	55	*	*
Ti(565mK)	8M	2600	2	NA	0.84	62.1	100	*	*
Ti(565mK)	2M	2800	2	NA	0.84	64.5	150	*	*
Ti(565mK)	1M	2100	2	NA	0.84	55.8	100	*	*

Table 1: Ti and Ir TES results. (Notes: NEP_{exp}: see Eq. (1). Band 6 has the largest absorber. T is scaled to predict τ_{Band6}. NA—P_{dark} was difficult to measure for the large G values of Ti TESs. *—τ for one Ti TES was 1.4ms and is assumed to represent a typical value for the other Ti TESs.)

Ultra-sensitive transition-edge sensors for the Background Limited Infrared/Sub-mm Spectrograph (BLISS) Instrument

This research was carried out at the Jet Propulsion Laboratory, California Institute of Technology, under a contract with the National Aeronautics and Space Administration.

REFERENCES

[1] J.C. Mather, *Applied Optics*, **21**, 1125 (1982).
[2] K.D. Irwin and G.C. Hilton, *Topics App. Phys.* **99**, 63 (2005).
[3] A.D.Beyer, M.E. Kenyon, P. M. Echternach, B.-H. Eom, J. Bueno, P.K. Day, J.J. Bock, and C.M. Bradford, *Proc. SPIE*, **7741**, 774121 (2010).
[4] M.Kenyon, P.K. Day, C.M. Bradford, J.J. Bock, and H.G. Leduc, *Proc. of 13th International Workshop on Low-Temperature Detectors*, 56 (2009).
[5] M.E. Kenyon, A.D. Beyer, P. M. Echternach, T. Chui, P.K. Day, J.J. Bock, W.A. Holmes, C.M. Bradford. *This conference's proceedings.* (2011).
[6] Piet A. J. de Korte, Joern Beyer, Steve Deiker, Gene C. Hilton, Kent D. Irwin, Mike MacIntosh, Sae Woo Nam, Carl D. Reintsema, Leila R. Vale, and Martin E. Huber. *Rev. Sci. Instr.* **74**, 3807 (2003).